Comparative Biochemistry and Physiology, Part B 251 (2021) 110511

Contents lists available at ScienceDirect

Comparative Biochemistry and Physiology, Part B

journal homepage: www.elsevier.com/locate/cbpb

The entomotoxin Jack Bean Urease changes cathepsin D activity in nymphs of the hematophagous insect *Dipetalogaster maxima* (Hemiptera: Reduviidae)

Natalia R. Moyetta [a,b], Leonardo L. Fruttero [a,b], Jimena Leyria [a,b], Fabian O. Ramos [a,b], Célia R. Carlini [c], Lilián Canavoso [a,b,*]

[a] Departamento de Bioquímica Clínica, Facultad de Ciencias Químicas, Universidad Nacional de Córdoba, Córdoba, CP 5000, Argentina
[b] Centro de Investigaciones en Bioquímica Clínica e Inmunología (CIBICI), Consejo Nacional de Investigaciones Científicas y Técnicas, Córdoba, CP 5000, Argentina
[c] Brain Institute (INSCER) and School of Medicine, Pontifícia Universidade Católica do Rio Grande do Sul, Porto Alegre, CEP 90610-000, Brazil

ARTICLE INFO

Keywords:
Cathepsin D
Urease
Triatomine
Mechanism of action
Toxicity

ABSTRACT

In insects, cathepsin D is a lysosomal aspartic endopeptidase involved in several functions such as digestion, defense and reproduction. Jack Bean Urease (JBU) is the most abundant urease isoform obtained from the seeds of the plant *Canavalia ensiformis*. JBU is a multifunctional protein with entomotoxic effects unrelated to its catalytic activity, by mechanisms not yet fully understood. In this work, we employed nymphs of the hematophagous insect *Dipetalogaster maxima* as an experimental model in order to study the effects of JBU on *D. maxima* CatD (DmCatD). In insects without treatment, immunofluorescence assays revealed a conspicuous distribution pattern of DmCatD in the anterior and posterior midgut as well as in the fat body and hemocytes. Western blot assays showed that the active form of DmCatD was present in the fat body, the anterior and posterior midgut; whereas the proenzyme was visualized in hemocytes and hemolymph. The transcript of *DmCatD* and its enzymatic activity was detected in the anterior and posterior midgut as well as in fat body and hemocytes. JBU injections induced a significant increase of DmCatD activity in the posterior midgut (at 3 h post-injection) whereas in the hemolymph, such an effect was observed after 18 h. These changes were not correlated with modifications in DmCatD mRNA and protein levels or changes in the immunofluorescence pattern. *In vitro* experiments might suggest a direct effect of the toxin in DmCatD activity. Our findings indicated that the tissue-specific increment of cathepsin D activity is a novel effect of JBU in insects.

1. Introduction

Cathepsin D (EC 3.4.23.5) is a soluble aspartic endopeptidase synthesized in the rough endoplasmic reticulum as pre-pro-cathepsin D (pre-pro-catD). After removal of the signal peptide, pro-CatD of about 52 kDa is carried to acidic vesicular intracellular structures, where afterwards it becomes a mature lysosomal peptidase. CatD activity can be regulated by several factors including pH and the interaction with other molecules such as specific inhibitors or glycosaminoglycans that promote its activation (Benes et al., 2008; Beckman et al., 2009). This enzyme participates in numerous physiological processes such as the metabolic degradation of polypeptide hormones and growth factors, the processing of enzyme activators and inhibitors as well as the regulation of programed cell death (Gacko et al., 2007). In insects, CatD has been implicated in food digestion (Padilha et al., 2009), defense against pathogens (Borges et al., 2006), cell remodeling associated with metamorphosis (Cho and Raikhel, 1992), yolk protein degradation (Fialho et al., 2005) and follicular atresia (Leyria et al., 2015), among others.

Abbreviations: BSA, bovine serum albumin; CatD, cathepsin D; DAPI, 4′,6-diamidino-2-phenylindole; DIC, differential interference contrast; DmCatD, *Dipetalogaster maxima* cathepsin D; JBU, Jack Bean Urease; NOS, nitric oxide synthase; pre-pro-catD, pre-pro-cathepsin D; OCT, Optimal Cutting Temperature; PBS, phosphate buffered saline; RFU, relative fluorescence units; UAP, UDP-*N*-acetylglucosamine pyrophosphorylase.

* Corresponding author at: Departamento de Bioquímica Clínica-CIBICI-CONICET, Facultad de Ciencias Químicas, Universidad Nacional de Córdoba, Haya de la Torre esq. Medina Allende s/n, Ciudad Universitaria, Córdoba, CP 5000, Argentina.
E-mail addresses: nmoyetta@fcq.unc.edu.ar (N.R. Moyetta), lfruttero@fcq.unc.edu.ar (L.L. Fruttero), jleyria@fcq.unc.edu.ar (J. Leyria), framos@fcq.unc.edu.ar (F.O. Ramos), celia.carlini@pucrs.br (C.R. Carlini), lcanavo@fcq.unc.edu.ar (L. Canavoso).

https://doi.org/10.1016/j.cbpb.2020.110511
Received 29 April 2020; Received in revised form 14 September 2020; Accepted 24 September 2020
Available online 29 September 2020

Dipetalogaster maxima is the largest of triatomine species, living in wild environments of Baja California Sur, Mexico (Guzmán-Bracho, 2001). Even though its epidemiological relevance as a vector of Chagas disease is nowadays limited, this species has started a process of adaptation to human dwellings. This aspect could be of sanitary significance in the near future, and deserves regular surveillance and monitoring (Salazar-Schettino et al., 2010). *D. maxima* has been used in our laboratory as a research model for the study of physiological aspects of the reproductive cycle, with special emphasis on the role of cathepsin D (DmCatD) during follicular atresia (Aguirre et al., 2011; Leyria et al., 2015). Although the activity of DmCatD was described in the fat body, ovaries and hemolymph of *D. maxima* females throughout the reproductive cycle, the expression and activity profile of DmCatD in nymphs has not been reported yet.

Ureases (urea amido hydrolases, EC 3.5.1.5.) are nickel-dependent enzymes that catalyse the hydrolysis of the urea into carbon dioxide and ammonia (Callahan et al., 2005; Kappaun et al., 2018). They are produced by a wide variety of organisms such as bacteria, fungi and plants but not by animals. Ureases are moonlighting proteins that exhibit a number of different functions besides their enzyme activity (Carlini and Ligabue-Braun, 2016). In the last decades, ureases were included alongside other molecules as defense proteins with biotechnological potential as insecticides (Staniscuaski and Carlini, 2012). The urease isoforms of the leguminous plant *Canavalia ensiformis* ("Jack Bean") were lethal when fed or injected to insect of different species, including phytophagous and hematophagous hemipterans (Carlini and Ligabue-Braun, 2016). Moreover, the injection of Jack Bean Urease (JBU), the most abundant urease isoform of *C. ensiformis*, into the hemocel of the triatomine *Rhodnius prolixus* triggered an immune response (Defferrari et al., 2014). Likewise, it was demonstrated that about 3% of the ingested JBU can withstand degradation in the midgut lumen and could be found intact later on in the insect hemolymph (Staniscuaski et al., 2010).

Insects display several mechanisms that provide the ability to adapt to situations presented by the contact with new environments and potentially natural or artificial toxic molecules (García-González et al., 2017). Within these mechanisms, the defense system of insects is part of a complex and dynamic response designed to cope with the harmful effects of some plant enzymes such as ureases (Staniscuaski and Carlini, 2012). Taking into account that the mechanisms of action of ureases in insects are not yet fully understood, we employed *D. maxima* as a model organism to study the effects of JBU on DmCatD.

2. Materials and methods

2.1. Chemicals

Rabbit polyclonal anti-human cathepsin D antibody (sc-10725) and MCF7 whole cell lysates (Santa Cruz Biotechnology, Palo Alto, CA, USA); Alexa Fluor 568-conjugated goat anti-rabbit IgG antibody and 4′,6-diamidino-2-phenylindole (DAPI) (Molecular Probes, Carlsbad, CA, USA); Tissue-Tek embedding medium Optimal Cutting Temperature (OCT, Miles, Elkhart, IN, USA); Fluorsave (Calbiochem, Darmstadt, Germany); electrophoresis protein standards (New England Biolabs, Ipswich, MA, USA); MMLV reverse transcriptase (Promega, Heidelberg, Germany); PCR Primers (Sigma Genosys, Houston, TX, USA); MasterPure RNA Purification Kit (Epicenter Biotechnologies, Madison, WI, USA); Power SYBR® Green PCR Master Mix (Applied Biosystems, Foster City, CA, USA) were from indicated commercial sources. Jack Bean Urease type C3, protease inhibitor cocktail for general use and all other chemicals were from Sigma-Aldrich (St. Louis, MO, USA). The fluorogenic peptide substrate Abz-AIKFFSAQ-EDDnp was synthetized by Dr. Maria Aparecida Juliano (Dept. Biophysics, Universidade Federal de São Paulo, Brazil).

2.2. Insects

The experiments were conducted with fed fifth instar nymphs of *D. maxima* (6–7 days after blood meal) and the blood meal represented approximately 6–7 times their own weight. The insects were taken from a colony maintained under standardized conditions (28 °C, 70% humidity, 8:16 h light:dark photoperiod) (Canavoso and Rubiolo, 1995), according to the recommendations of the National Institute of Parasitology (National Health Ministry, Argentina) (Núñez and Segura, 1987).

2.3. Ethics statement

The maintenance of the insect colony followed a protocol (Res. Dec. #1392/2016-EXP-UNC:0034722/2016) authorized by the Animal Care Committee of the Centro de Investigaciones en Bioquímica Clínica e Inmunología (CIBICI-CONICET-Universidad Nacional de Córdoba) in accordance with the guidelines of the Canadian Council on Animal Care with the assurance number A5802-01 delivered by the Office of Laboratory Animal Welfare (National Institutes of Health). The animal facility at the CIBICI-CONICET belongs to the Argentine National Ministry of Science (Sistema Nacional de Bioterios, MINCyT, http://www.bioterios.mincyt.gob.ar).

2.4. RNA extraction and reverse transcription/quantitative PCR (RT-qPCR)

The fat bodies, the anterior and posterior midguts were individually dissected in cold phosphate buffered saline (PBS: 6.6 mM Na_2HPO_4/KH_2PO_4, 150 mM NaCl, pH 7.4). The hemolymph was collected from an incision in one of the legs and stored in ice cold microtubes containing anticoagulant solution (10 mM Na_2EDTA, 100 mM glucose, 62 mM NaCl, 30 mM sodium citrate, 26 mM citric acid, pH 4.6) at a ratio of 1:5 (anticoagulant: hemolymph) and phenylthiourea to avoid melanization (Fruttero et al., 2016). The hemolymph from three insects was pooled and centrifuged at 1000 × *g* for 10 min at 4 °C to pellet the hemocytes.

RNA extraction of tissue samples and hemocytes was conducted employing the NucleoSpin RNA XS kit (Macherey-Nagel, GmbH & Co, Düren, Germany) following the instructions from the manufacturer. cDNA was synthesized from 2 μg of total RNA by means of reverse transcription reaction employing the MMLV reverse transcriptase protocol. Real time PCR (qPCR) analysis was performed using an ABI Prism 7500 sequence detection system (Applied Biosystems, Foster City, CA, USA) and SYBR green chemistry as already described (Leyria et al., 2015). The $2^{-\Delta\Delta Ct}$ method was used to quantify relative changes in gene expression using 18S ribosomal RNA (18S rRNA) as normalizer. The primer sequences are depicted in Supplementary Table S1.

2.5. Analysis of DmCatD expression by Western blot

The fat bodies, the anterior and posterior midguts were dissected and stored with a protease inhibitor cocktail at −80 °C until use. Thereafter, the organs were individually homogenized in buffer Tris-HCl-Na_2EDTA (50 mM Tris, 1 mM EDTA, 0.1% Triton X-100, pH 7.5) and centrifuged at 1000 × *g* for 10 min (4 °C). The supernatant was recovered and subjected to a second spin at 20,000 × *g* for 20 min at the same temperature. The protein concentration was measured in the second supernatant according to Bradford (1976). The hemolymph samples were individually collected as described above and centrifuged at 1000 × *g* for 10 min at 4 °C. The supernatant was labeled as hemocyte-free hemolymph and the pellet (hemocytes) was resuspended in buffer sample. Then, samples were electrophoresed in 15% SDS-PAGE, transferred to a nitrocellulose membrane and blocked, according to Leyria et al. (2015). After washing, the membrane was incubated with the polyclonal anti-cathepsin D antibody (1:300 dilution) overnight at 4 °C and then with the secondary antibody (Li-Cor IRDye 800CW polyclonal goat anti-rabbit IgG, 1:15,000) at room temperature for 1 h. Blots were analysed with the

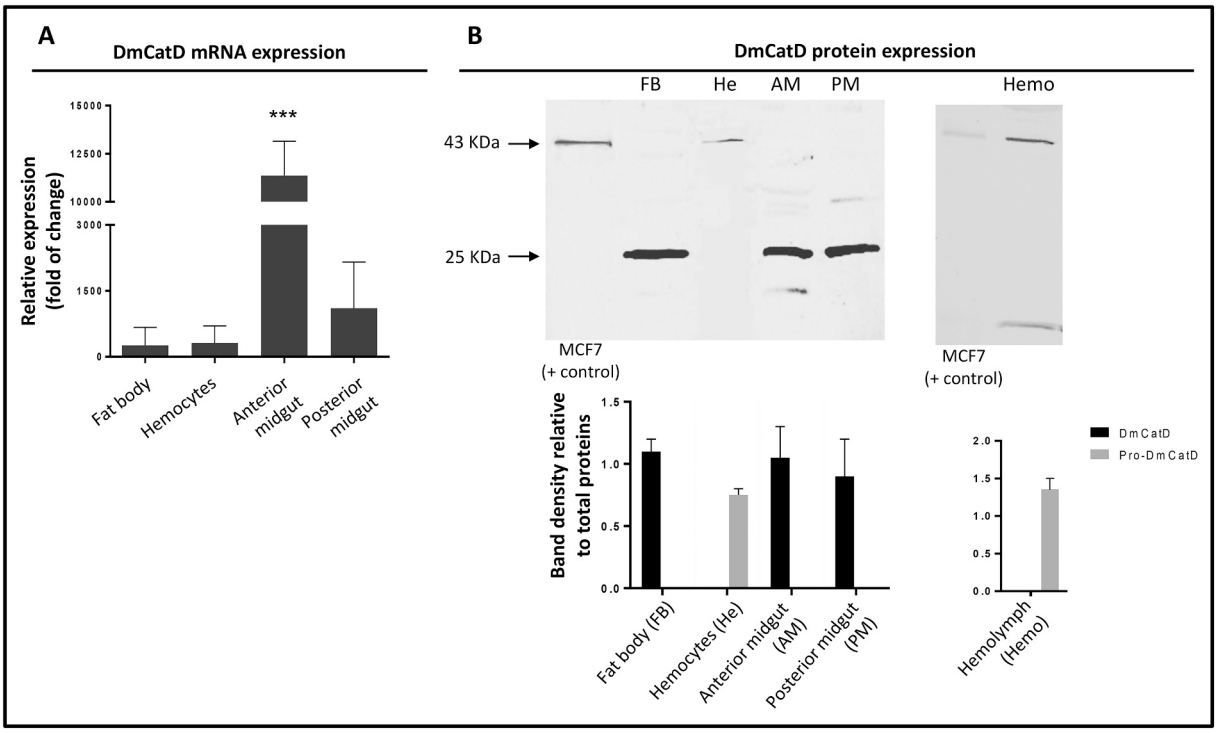

Fig. 1. DmCatD expression profile (mRNA and protein) in fifth instar nymphs of *D. maxima*. The anterior (AM) and posterior midgut (PM), the fat body (FB), the Hemocytes (He) and the hemolymph (Hemo) from fed nymphs were processed for qPCR (A) and Western blot (B), as described in Materials and Methods. For qPCR, total RNA was extracted and the DmCatD transcripts were quantified using specific primers and 18S ribosomal RNA as normalizer. ***$P < 0.0001$ *vs* fat body, hemocytes and posterior midgut ($n = 5$). For Western blot, approximately 50 μg of proteins were loaded in each lane, separated by 15% SDS-PAGE and probed with the anti-CatD antibody. Whole cell MCF7 lysate (0.2 μg) was employed as a positive control. Densitometric analyses of three independent blots were performed upon the intensity of the pro-DmCatD and DmCatD bands detected in each lane and the amount of total proteins loaded and stained with Ponceau S.

Odyssey quantitative Western blot near-infrared system (Li-Cor Biosciences, Lincoln, NE, USA) using default settings. MCF7 whole cell lysate derived from the MCF cell line was used as a positive control of Western Blot assays (Leyria et al., 2015, 2018).

2.6. Determination of DmCatD activity

The activity of DmCatD was measured in samples obtained as described in the previous section using the specific synthetic fluorogenic substrate Abz-AIKFFSAQ-EDDnp, according to Aguirre et al. (2011) with minor modifications. For these experiments the material was homogenized in PBS. Reactions were monitored every 6 s for 5 min in a Multi-Mode Microplate Reader Sinergy HT (BioTek Instruments, Winooski, VT, USA) with 320/430 nm excitation/emission filters. Results were expressed as relative fluorescence units (RFU)/μg protein/min.

For *in vitro* experiments, aimed to investigate a direct effect of JBU on DmCatD activity, 30 μg of protein of posterior midgut homogenates and hemocyte-free hemolymph were incubated with 1 and 100 nM JBU (540 kDa) or an equivalent volume of PBS (control) for 1 h at room temperature and immediately employed for enzyme activity assays. An additional control incubating JBU plus the fluorogenic substrate was also performed. No CatD-like enzymatic activity was found (data not shown).

2.7. Immunofluorescence assays

Fat bodies, anterior and posterior midguts were dissected out and subjected to cryostat sectioning as described (Leyria et al., 2015). The hemolymph was collected as described and the hemocytes were adhered to poly-L-lysine-treated slides according to Moyetta et al. (2017). The slides were permeabilized and blocked in 0.1% Triton X-100, bovine serum albumin (BSA) 2.5%, fetal bovine serum 5% in PBS for 1 h at room temperature, followed by incubations with the polyclonal anti-cathepsin D antibody (1:25) and the anti-rabbit IgG labeled with Alexa Fluor® 568 (1:300) for 1 h at 37 °C each. Antibodies were diluted in 1% BSA in PBS and all incubations were performed in a humid chamber. Slides were washed twice with PBS for 5 min and controls of the immunofluorescence assays were carried out without the incubation of one or both antibodies. The nuclei were stained with 300 nM DAPI for 2 min and the slides were mounted in Fluorsave and observed with a Leica DMi8 microscope (Leica Microsystems, Wetzlar, Germany).

2.8. Injections of JBU into the hemocel of D. maxima nymphs

Insects were placed ventral side up under a stereoscopic microscope and injections of JBU (0.125 μg/mg insect body weight) in PBS were performed using a microsyringe. Controls were carried out by injecting equivalent volumes of PBS (Fruttero et al., 2016).

2.9. Gel shift and Western blot

In order to explore the possibility of proteins that can interact *in vitro* with JBU, a combination of gel shift and Western blot was employed (Bollag and Edelstein, 1991; Park and Raines, 1997). JBU alone (0.5 μg) or mixed with posterior midgut homogenates or hemocyte-free hemolymph (50 μg each) were incubated for 1 h at room temperature and subjected to a 6% polyacrylamide gel electrophoresis under non denaturing conditions. Then, samples were transferred to a nitrocellulose membrane and blocked. After washing, the membrane was incubated with the polyclonal anti-Jaburetox antibody (1:1000 dilution) for 1 h at room temperature and then with the secondary antibody as described above. Jaburetox is a recombinant JBU-derived peptide (Mulinari et al., 2007) and the cross reactivity of the antibody with the JBU was already reported (Martinelli et al., 2017).

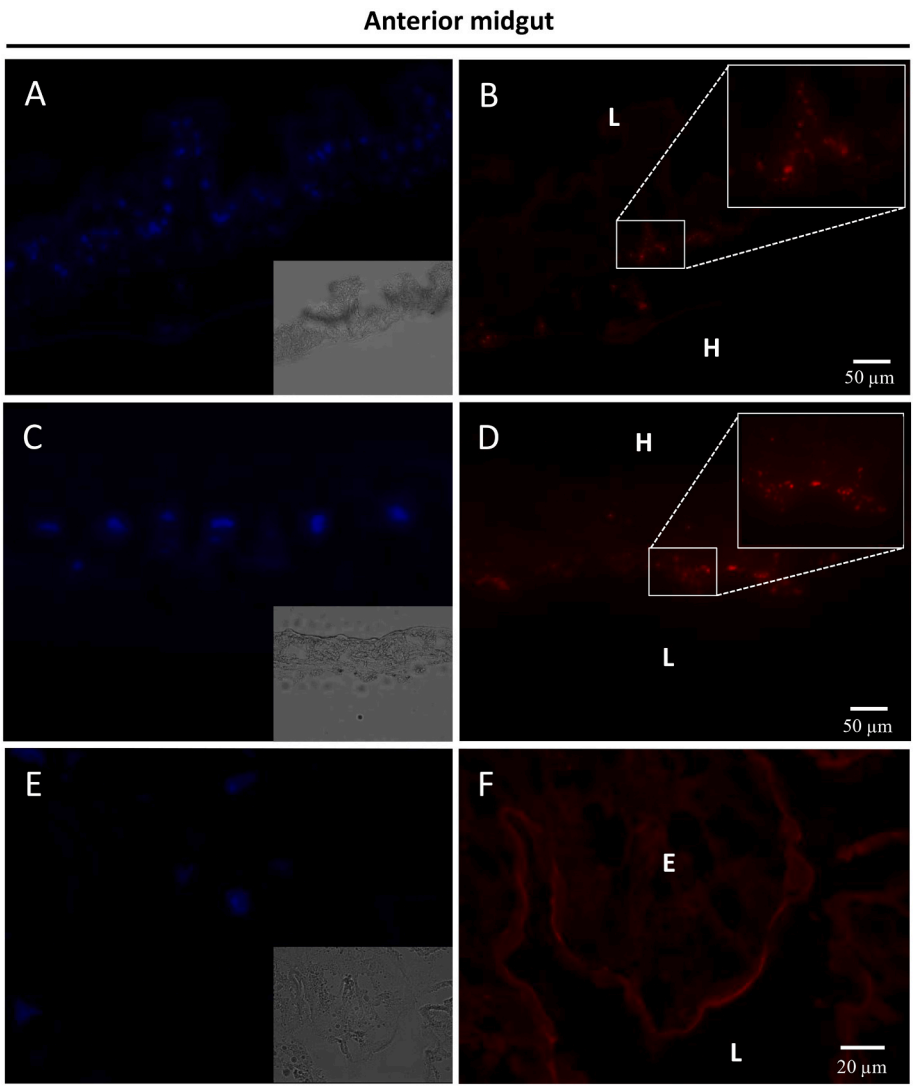

Fig. 2. DmCatD distribution in the anterior midgut of *D. maxima* nymphs at 6 days after blood meal. The organs were dissected and processed as described in the Materials and Methods section. Cryostat sections were incubated with an anti-cathepsin D antibody, an Alexa Fluor 568-conjugated secondary antibody (red) and DAPI (blue) in order to stain the nuclei. (A, C and E) are the fluorescence nuclei images of different sections while (B, D and F) are the corresponding fluorescent profiles of DmCatD. Insets show the matching differential interference contrast (DIC) images. H, hemolymph; L, lumen; E, epithelium. Bars: 50 µm for A–D and 20 µm for *E*–F. (For interpretation of the referencems to colour in this figure legend, the reader is referred to the web version of this article.)

2.10. Statistical analysis

For Western blot, qPCR and enzymatic assays, samples from anterior and posterior midgut, fat body and hemolymph were individually collected and then processed as stated. In addition, assays with hemocytes were performed by pooling the hemolymph from 3 insects for each sample. Student's *t*-test or one-way ANOVA were used and a P value <0.05 was considered statistically significant. Graphs and statistical tests were performed using software program GraphPad Prism 5 (San Diego, CA, USA) and the data was expressed as mean ± Standard Error of the Mean (SEM).

3. Results and discussion

3.1. DmCatD expression

The transcription profile of DmCatD was assessed by qPCR in fat bodies, hemocytes as well as in the anterior and posterior midguts of *D. maxima* nymphs at 6–7 days after a blood meal (Fig. 1A). The DmCatD transcript was detected in all assayed samples, with the highest expression found in the anterior midgut (Fig. 1A). This result was expected, taking into account the ubiquitous distribution of CatD (Benes et al., 2008). When the obtained amplicons were submitted to sequencing, BLAST searches retrieved cathepsin D from *Triatoma infestans* (a related triatomine species) and *D. maxima*, thus confirming the identity of amplified products (Supplementary Table S2). The data presented in Supplementary Table S2 summarized the results for identification of PCR products in hemocytes and midgut. Data on the related fat body amplicons, assessed previously by Leyria et al. (2015) were not included. Balczun et al. (2012) described two CatD genes in *T. infestans* and Pimentel et al. (2017) reported 10 CatD genes in the hemipteran *Dysdercus peruvianus*. However, we were able to amplify only one DmCatD gene, similar to what was reported in other insect species (Gui et al., 2006; Kang et al., 2017). Balczun et al. (2012) observed in *T. infestans* that CatD genes were expressed in the anterior and posterior midgut but not in the rectum, salivary glands, Malpighian tubules and hemocytes of nymphs. However, as shown in Fig. 1A, hemocytes of *D. maxima* nymphs expressed the DmCatD transcript. Such a result could be explained either by interspecific differences or by the different technical protocols employed.

When DmCatD was analysed by Western blot (Fig. 1B), an immunoreactive band compatible with the active form of DmCatD (~25 kDa) was visualized in the fat body and in the anterior and posterior midguts. Taking into account that both midgut divisions showed a similar high expression of DmCatD (Fig. 1B) and considering that in triatomines, cathepsins have been involved with the digestion mainly in the posterior midgut, it was rather unexpected to find such a high expression of the DmCatD in the anterior midgut of *D. maxima* (Balczun et al., 2012). In

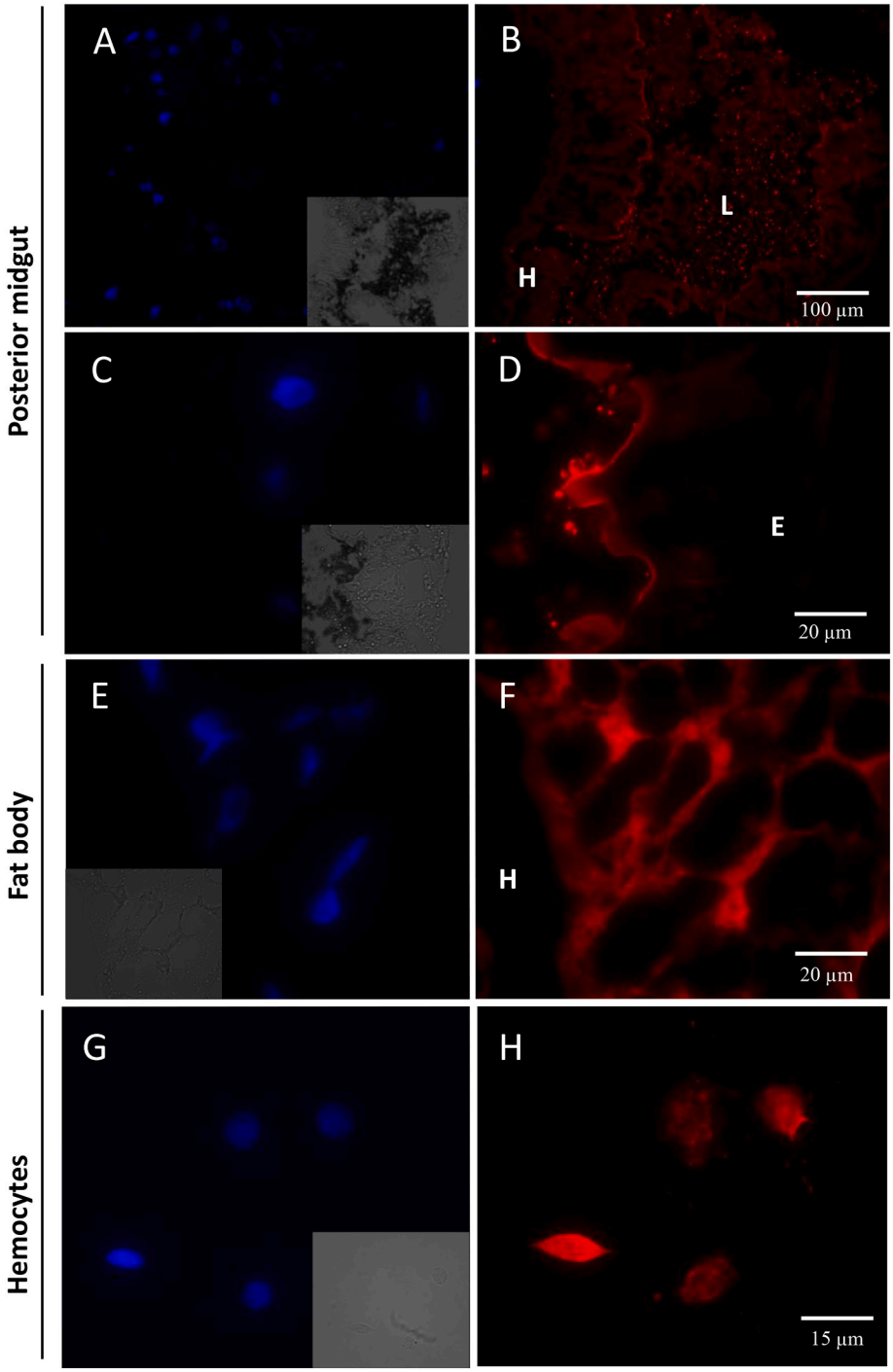

Fig. 3. DmCatD distribution in the posterior midgut and DmCatD immunofluorescence profile in the posterior midgut, fat body and hemocytes of *D. maxima* nymphs. Cryostat sections were incubated with the anti-cathepsin D antibody, the Alexa Fluor 568-conjugated secondary antibody and DAPI to stain the nuclei. (A and C) show the nuclei of different posterior midgut sections while (B and D) are the corresponding fluorescent patterns of DmCatD. (E and G) display the nuclei from fat body sections and hemocyte preparations, respectively, while (F and H) are the respective DmCatD fluorescent profiles. Insets show the corresponding DIC images. H, hemolymph; L, lumen; E, epithelium. Bars: 100 µm for A–B, 20 µm for C–F and 15 µm for G–H.

the context of the physiology of digestive system, future approaches are necessary to evaluate this issue. It is important to highlight that, even though DmCatD transcriptional expression was significantly higher in the anterior midgut compared to that of the posterior midgut, no difference at the level of protein expression was observed (Fig. 1). On the other hand, only one band of about 43 kDa compatible with the pro-enzyme, pro-DmCatD, was present in hemocytes and hemocyte-free hemolymph (Fig. 1B). In line with this finding, fed adult females of *D. maxima* showed a hemolymph profile in which only pro-DmCatD was detected (Leyria et al., 2015).

3.2. DmCatD in tissues of D. maxima

Indirect immunofluorescence assays were conducted in order to analyse the distribution of DmCatD in different tissues as well as in the hemocytes of fifth instar nymphs. The specificity of the polyclonal antibody employed was previously demonstrated (Leyria et al., 2015, 2018). DmCatD signal displayed an even distribution in the fat body, anterior and posterior midguts and hemocytes (Figs. 2–3). In the case of the midgut divisions, the fluorescence pattern for DmCatD was evidenced in the apical region of the anterior and posterior midgut (Figs. 2F, 3D). DmCatD was also observed in the midgut lumen (Fig. 3B), likely indicating that the enzyme was secreted into this compartment. This finding is in agreement with the role of CatD in the extracellular

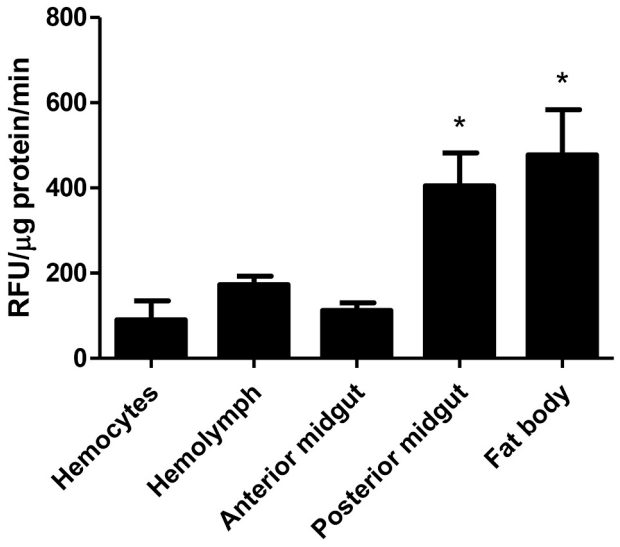

Fig. 4. DmCatD activity in fifth instar nymphs of *D. maxima*. The anterior and posterior midgut, the fat body, the hemocytes and the hemolymph from fed nymphs were processed for enzyme activity assays as described in Materials and Methods. DmCatD activity was determined using a fluorogenic substrate and expressed as relative fluorescence units (RFU) by microgram of protein by min. $^{*}P < 0.05$ *vs* anterior midgut, hemocytes and hemolymph ($n = 4$).

digestion in the midgut lumen as already demonstrated for triatomines and other hematophagous insects (Santiago et al., 2017). The fluorescence corresponding to DmCatD was detected in the cytoplasm of the fat body cells and the hemocytes (Fig. 3G). The presence of DmCatD in the cytoplasm of fat body cells was also observed in *D. maxima* adult females (Leyria et al., 2015), where it seems to be involved in the remodeling of the tissue in response to specific metabolic requirements. On the other hand, the hemocytes presented a variable immunofluorescence pattern (Fig. 3H) that could be due to the presence of different hemocyte types fulfilling diverse functions in this insect species.

3.3. DmCatD activity in tissues and hemolymph

As shown in Fig. 4, the fat body and the posterior midgut of *D. maxima* nymphs presented high levels of DmCatD activity, even though the protein expression was similar in the anterior and posterior midgut (Fig. 1B). The enzymatic activity was also demonstrated in hemocytes, hemolymph and in the anterior midgut. Leyria et al. (2015) reported the DmCatD activity profile in females, which showed high levels in the fat bodies and comparatively lower levels in the hemolymph. Several investigations in Hemiptera described that CatD is highly expressed in the midgut, in line with its digestive function in the midgut lumen (Borges et al., 2006; Balczun et al., 2012; Pimentel et al., 2017). Cathepsin D activity in the midgut of triatomines was firstly demonstrated by Houseman and Downe (1980) in *R. prolixus*. In contrast to the results of Balczun et al. (2012) in *T. infestans*, DmCatD activity was also present in hemocytes, supporting the functional role of the enzyme in these cells.

3.4. JBU effects on DmCatD

With the aim of studying the entomotoxic effect of the JBU and a potential interference on DmCatD, fifth instar nymphs of *D. maxima* were injected with PBS or with JBU at 0.125 µg/mg insect body weight, a dose previously reported as lethal to other triatomine species (Defferrari et al., 2014). The experiments carried out to monitor the survival of insects showed no mortality in controls or JBU-injected insects along a 7-day period (results not shown). It was also observed that JBU elicited a significant increment of DmCatD activity in the whole midgut homogenates (Fig. S1). Taking into account that, from a morphological and physiological point of view the intestine of triatomines is composed by the anterior midgut (also termed stomach) and by the small intestine, commonly termed posterior midgut (Schaub, 2009), the effects of the entomotoxin in the remaining approaches were analysed in the anterior and posterior midgut divisions separately, instead of the whole midgut. As depicted in Fig. 5A–B, the posterior midgut and the fat body of PBS- and JBU-injected insects presented the highest DmCatD activity levels at 3 and 18 h post-injection. These profiles were similar to those observed in non-injected insects (Fig. 4). In contrast, in the hemocytes as well as in the anterior midgut and fat body, treatment of the nymphs with JBU did not cause significant changes in the enzymatic activity, when compared to that in control insects (Fig. 5A–B).

Injection of JBU into the insects' hemocel induced a significant increase in DmCatD activity in the posterior midgut at 3 h post-injection, subsequently decreasing to basal levels at 18 h thereafter. On the other hand, in the hemolymph of JBU-injected insects the activity of DmCatD showed significant increase only 18 h post-injection (Fig. 5A–B). However, such effects did not correlate with increases in the DmCatD transcript levels in the posterior midgut as well as in the intensity of immunoreactive bands compatible with DmCatD or pro-DmCatD in the midgut and hemolymph, respectively (Fig. 5C–D). Moreover, the JBU injection did not elicit modifications in the DmCatD immunofluorescence pattern in the posterior midgut (Fig. 6). As discussed above, the posterior midgut has a role in digestion, thus, it is probable that the increment in DmCatD activity upon JBU treatment might enhance the availability of nutrients, and then rendering the insect more fitted to withstand the toxin challenge. Taking into account that CatD has a role in the innate immunity of insects and vertebrates (Conus and Simon, 2010; Saikhedkar et al., 2015), the increase in DmCatD activity in the midgut and hemolymph could be part of the insect's immune response to the JBU.

Since there are reports describing the involvement of CatD in cell death (Gui et al., 2006; Aguirre et al., 2013; Zhang et al., 2018), we wonder if the increase in DmCatD activity induced by JBU in the posterior midgut could be linked to autophagy and/or apoptosis. Immunofluoresence patterns against markers of these mechanisms of cell death revealed no differences in the posterior midgut of JBU and PBS-injected insects (results not shown). Thus, in our experimental conditions, it seems unlikely that the activation of DmCatD by JBU could be associated with autophagy and apoptosis.

The change on DmCatD activity elicited by the injection of JBU was reproduced *in vitro* by incubating the entomotoxin with the posterior midgut homogenates but not with hemocyte-free hemolymph. In this sense, 100 nM JBU significantly increased the DmCatD activity in the posterior midgut (Fig. 7), suggesting a direct effect of the entomotoxin on the enzyme. Contrarily, incubations with either 1 or 100 nM JBU, did not significantly modify the enzyme activity in the hemolymph (Fig. 7), strongly suggesting a tissue-specific effect of JBU. When midgut homogenates and hemocyte-free hemolymph were combined to explore the presence of CatD inhibitor(s) that would explain the lack of JBU effect on DmCatD activity in the hemolymph, no decrease in such enzymatic activity was found (results not shown). It is worth mentioning that for these assays, the activity of DmCatD was induced by the incubation of the homogenates containing the enzyme in an acidic medium, allowing the autocatalytic activation of the pro-enzyme to form the mature DmCatD, which carried out the cleavage of the synthetic fluorogenic substrate (Leyria et al., 2015; Stoka et al., 2016). Thus, the tissue-specific *in vitro* effect elicited by JBU on the enzyme activity could be related to the status of the enzyme (Fig. 7), since the active form of DmCatD was mainly expressed in the posterior midgut whereas only pro-DmCatD was detected in the hemolymph (Fig. 1). The fact that JBU induces an increase in DmCatD activity without altering its expression or transcript levels suggests that the toxin interacts with the enzyme or other proteins, leading to a conformational change in DmCatD rendering it more active. However, in our experimental conditions, when a gel

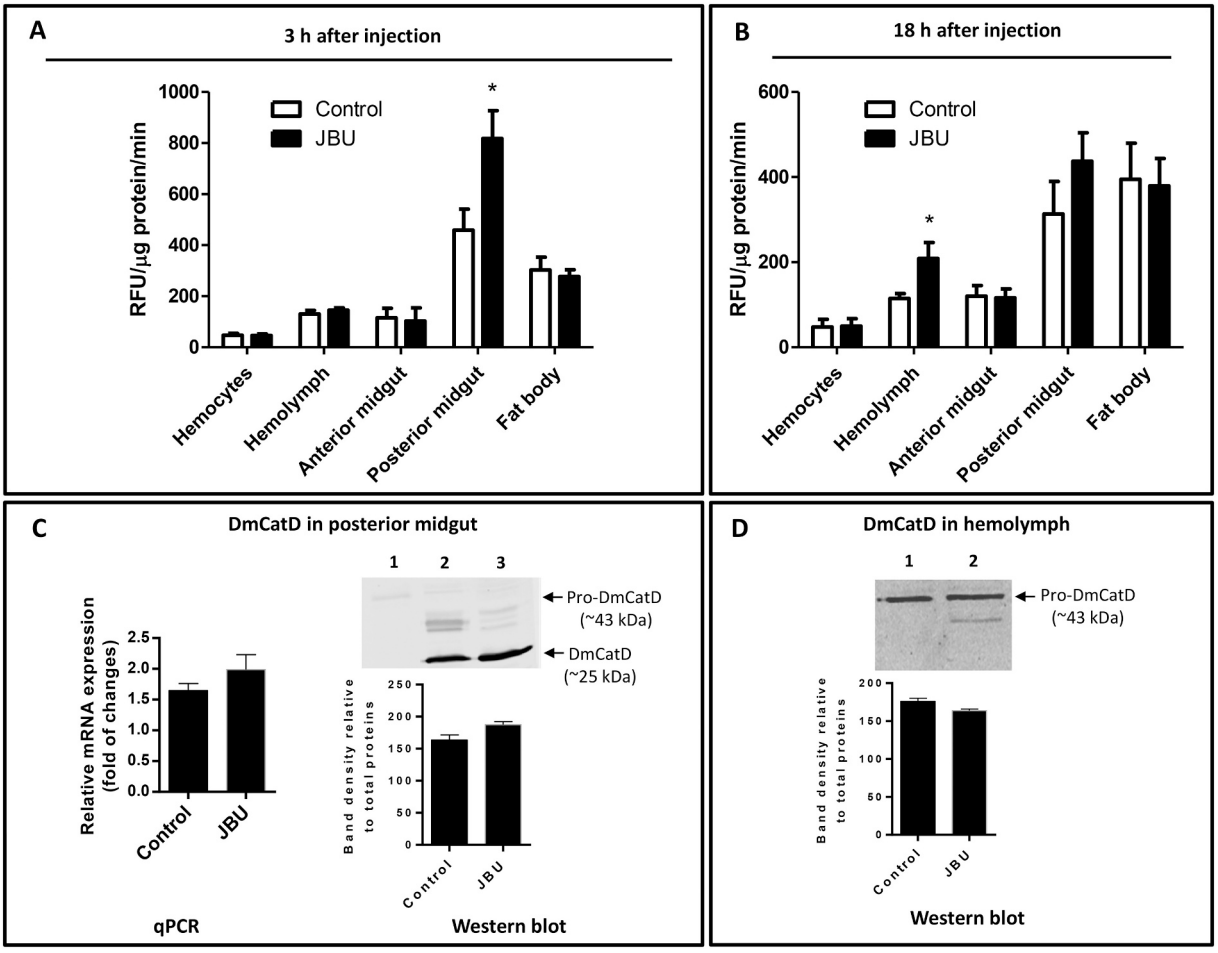

Fig. 5. Effect of Jack Bean Urease (JBU) treatment on DmCatD activity in fifth instar nymphs of *D. maxima*. Insects were injected with PBS (controls) or with JBU (0.125 µg/mg of body weight) and at 3 (A) and 18 h (B) after injection, different tissues and cells were collected, homogenized and processed as described in Materials and Methods. DmCatD activity was determined using a fluorogenic substrate and expressed as relative fluorescence units (RFU) by microgram of protein by min. $^*P < 0.05$ *vs* control ($n = 6$). Samples obtained at 3 h after injection from posterior midgut (A) and at 18 h from hemolymph (B) were processed for qPCR and Western blot, as depicted in the figure.

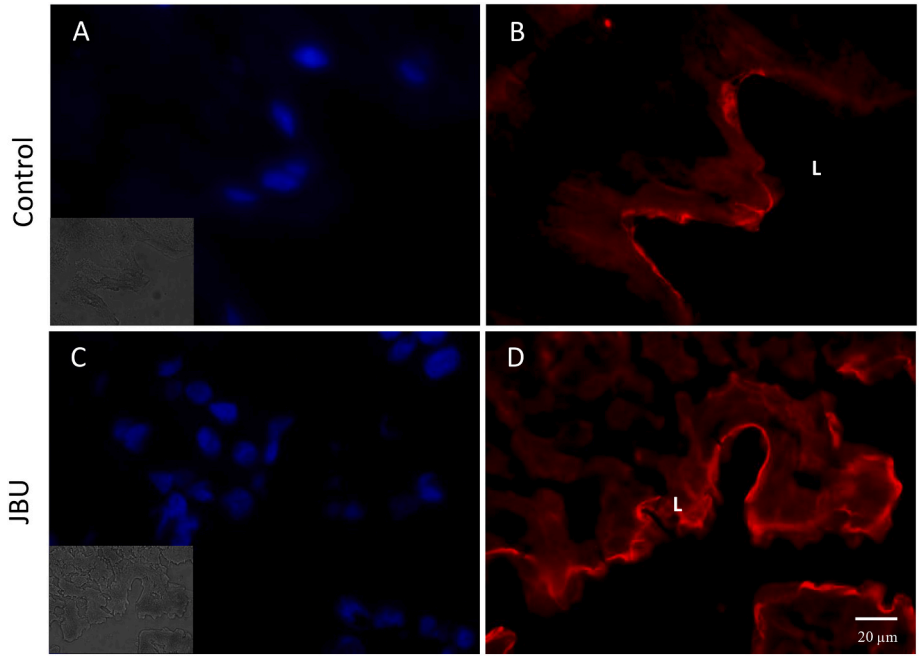

Fig. 6. Effect of Jack Bean Urease (JBU) treatment on DmCatD distribution on posterior midgut of *D. maxima*. Insects were injected with PBS (A–B, controls) or with JBU (C–D, 0.125 µg/mg of body weight) and at 3 h after injection, the posterior midguts were dissected processed for immunofluorescence as described in Materials and Methods. Cryostat sections were incubated with the anti-cathepsin D antibody, the Alexa Fluor 568-conjugated secondary antibody (red) and DAPI (blue). A and C are the fluorescence nuclei images of different sections while B and D are the corresponding fluorescent profiles of DmCatD. Insets show the matching DIC images. H, hemolymph; L, lumen; E, epithelium. Bars: 20 µm. (For interpretation of the references to colour in this figure legend, the reader is referred to the web version of this article.)

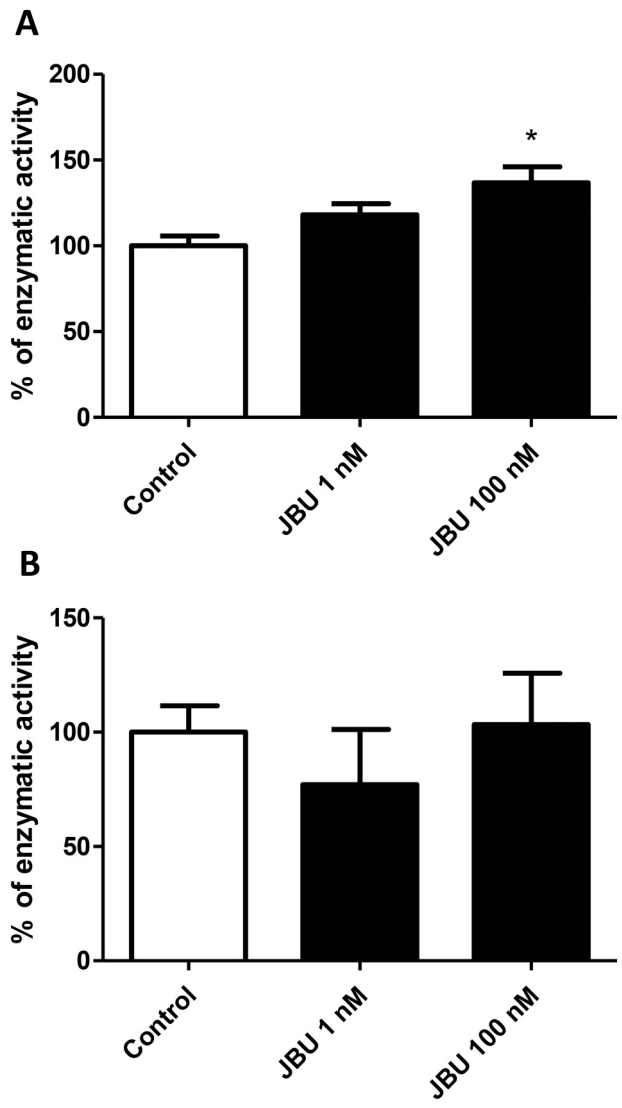

Fig. 7. *In vitro* effect of Jack Bean Urease (JBU) on DmCatD activity in the posterior midgut and hemolymph of *D. maxima*. Posterior midgut homogenates (A) and hemocyte-free hemolymph (B) were incubated for 1 h at room temperature with the indicated JBU concentrations or buffer for the controls. DmCatD activity was determined using the fluorogenic substrate and expressed as % of enzymatic activity, taking the control as 100%. *$P < 0.05$ *vs.* control ($n = 4$).

shift assay followed by Western blot was carried out after *in vitro* incubation of JBU with either the posterior midgut homogenates or hemolymph, no changes in the aggregation states of the native JBU were observed, supporting thus the absence of such interactions (Fig. S2).

It was previously demonstrated that JBU as well as Jaburetox, which is a recombinant JBU-derived peptide (Mulinari et al., 2007), affected the activity of several enzymes in a tissue-specific fashion. Thus, Jaburetox elicited changes in the activity of nitric oxide synthase (NOS) and UDP-*N*-acetylglucosamine pyrophosphorylase (UAP) in the central nervous system, salivary glands and hemocytes of *R. prolixus* (Fruttero et al., 2017; Moyetta et al., 2017). Moreover, JBU altered the enzyme activity of UAP in the salivary glands and in the fat body of *R. prolixus* (Krug, 2016). It also modulated the activity of acetyl cholinesterase, a target of several insecticides, in the whole head and in the central nervous tissue of *N. cinerea* (Carrazoni et al., 2016; Perin, 2018).

4. Conclusions

This work is a novel report of DmCatD expression in nymphs of the triatomine *D. maxima* and provides the first evidence that cathepsin D is a molecular target of JBU, the main urease isoform. We showed that the injection of a non-lethal dose of JBU induced an early increase in DmCatD activity in the posterior midgut and later on, in the hemolymph. In this sense, DmCatD activation in the midgut could be relevant in maximizing blood protein digestion to promote higher availability of nutrients to withstand the JBU toxic effect. In addition, the changes in CatD activity detected in the midgut and the hemolymph have to be interpreted in the context of insect immunity, since the enzyme not only displays a well-known role in the insect immune response (Borges et al., 2006; Saikhedkar et al., 2015) but also, in terms of the immune response elicited by JBU which might mimic a pathogenic infection (Defferrari et al., 2014; Fruttero et al., 2016).

Interestingly, DmCatD *in vivo* activation was not mediated by increased mRNA levels and protein expression but it was triggered *in vitro* in midgut homogenates, suggesting a direct effect of the toxin upon the enzyme. However, the experimental approach employed does not support such a possibility. The fact that DmCatD is found on its active form in the midgut and as pro-enzyme in the hemolymph could explain their different patterns of *in vitro* activation. In summary, our finding bring additional knowledge of the JBU action mechanism and add another level of complexity to their repertoire of toxic effects.

Supplementary data to this article can be found online at https://doi.org/10.1016/j.cbpb.2020.110511.

Declaration of Competing Interest

The authors declare that they have no known competing financial interests or personal relationships that could have appeared to influence the work reported in this paper.

Acknowledgements

The authors thank Raúl Stariolo (Coordinación Nacional de Control de Vectores, Córdoba, Argentina) for assistance in the insect facility care. L.E.C. and L.L.F. are members of the National Research Council (CONICET, Argentina). Work in the L.E.C. laboratory is supported by grants from SECyT-UNC (CONSOLIDAR 2018-21), FONCyT (PICT 2016-1351), and CONICET (PIP 0159). Work in CRC is supported by the Brazilian agencies: Conselho Nacional de Desenvolvimento Científico e Tecnológico (CNPq) [proj. 47.5908/2012 and 446052/2014-1]; Coordenação de Aperfeiçoamento de Pessoal de Nível Superior (CAPES) [Finance Code 001, Edital Toxinologia 63/2010 proj. 1205/2011, Edital Pesquisador Visitante–PVE 054/2012, Science Without Borders, and Portal de Periódicos]; Fundação de Amparo à Pesquisa do Estado do Rio Grande do Sul (FAPERGS, Edital PRONEX, proj. 10/0014-2).

References

Aguirre, S.A., Fruttero, L.L., Leyria, J., Defferrari, M.S., Pinto, P.M., Settembrini, B.P., Rubiolo, E.R., Carlini, C.R., Canavoso, L.E., 2011. Biochemical changes in the transition from vitellogenesis to follicular atresia in the hematophagous *Dipetalogaster maxima* (Hemiptera: Reduviidae). Insect Biochem. Mol. Biol. 42, 832–841.

Aguirre, S.A., Pons, P., Settembrini, B.P., Arroyo, D., Canavoso, L.E., 2013. Cell death mechanisms during follicular atresia in *Dipetalogaster maxima*, a vector of Chagas' disease (Hemiptera: Reduviidae). J. Insect Physiol. 59, 532–541.

Balczun, C., Siemanowski, J., Pausch, J.K., Helling, S., Marcus, K., Stephan, C., Meyer, H. E., Schneider, T., Cizmowski, C., Oldenburg, M., Höhn, S., Meiser, C.K., Schuhmann, W., Schaub, G.A., 2012. Intestinal aspartate proteases TiCatD and TiCatD2 of the haematophagous bug *Triatoma infestans* (Reduviidae): sequence characterisation, expression pattern and characterisation of proteolytic activity. Insect Biochem. Mol. Biol. 42, 240–250.

Beckman, M., Freeman, C., Parish, C.R., Small, D.H., 2009. Activation of cathepsin D by glycosaminoglycans. FEBS J. 276, 7343–7352.

Benes, P., Vetvicka, V., Fusek, M., 2008. Cathepsin D: many functions of one aspartic protease. Crit. Rev. Oncol. Hematol. 68, 12–28.

Bollag, D.M., Edelstein, S.J., 1991. Electrophoresis under nondenaturing conditions. In: Protein Methods. Wiley-Liss Inc., New York, pp. 143–160.
Borges, E.C., Machado, E.M., García, E.S., Azambuja, P., 2006. *Trypanosoma cruzi*: effects of infection on cathepsin D activity in the midgut of *Rhodnius prolixus*. Exp. Parasitol. 112, 130–133.
Bradford, M.M., 1976. A rapid and sensitive method for the quantitation of micrograms quantities of protein utilizing the principle of protein-dye binding. Anal. Biochem. 72, 248–254.
Callahan, B.P., Yuan, Y., Wolfenden, R., 2005. The burden borne by urease. J. Am. Chem. Soc. 127, 10828–10829.
Canavoso, L.E., Rubiolo, E.R., 1995. Interconversions of lipophorin particles by adipokinetic hormone in hemolymph of *Panstrongylus megistus*, *Dipetalogaster maximus* and *Triatoma infestans* (Hemiptera: Reduviidae). Comp. Biochem. Physiol. 112A, 143–150.
Carlini, C.R., Ligabue-Braun, R., 2016. Ureases as multifunctional toxic proteins: a review. Toxicon 110, 90–109.
Carrazoni, T., de Avila Heberle, M., Perin, A.P., Zanatta, A.P., Rodrigues, P.V., Dos Santos, F.D., de Almeida, C.G., Vaz Breda, R., Dos Santos, D.S., Pinto, P.M., da Costa, J.C., Carlini, C.R., Dal Belo, C.A., 2016. Central and peripheral neurotoxicity induced by the Jack Bean Urease (JBU) in *Nauphoeta cinerea* cockroaches. Toxicology 368-369, 162–171.
Cho, W.L., Raikhel, A.S., 1992. Cloning of cDNA for mosquito lysosomal aspartic protease. Sequence analysis of an insect lysosomal enzyme similar to cathepsins D and E. J. Biol. Chem. 267, 21823–21829.
Conus, S., Simon, H.-U., 2010. Cathepsins and their involvement in immune responses. Swiss Med. Wkly. 140, w13042.
Defferrari, M.S., da Silva, R., Orchard, I., Carlini, C.R., 2014. Jack bean (*Canavalia ensiformis*) urease induces eicosanoid-modulated hemocyte aggregation in the Chagas' disease vector *Rhodnius prolixus*. Toxicon 82, 18–25.
Fialho, E., Nakamura, A., Juliano, L., Masuda, H., Silva-Neto, M.A., 2005. Cathepsin D-mediated yolk protein degradation is blocked by acid phosphatase inhibitors. Arch. Biochem. Biophys. 436, 246–253.
Fruttero, L.L., Moyetta, N.R., Uberti, A.F., Grahl, M.V., Lopes, F.C., Broll, V., Feder, D., Carlini, C.R., 2016. Humoral and cellular immune responses induced by the urease-derived peptide Jaburetox in the model organism *Rhodnius prolixus*. Parasit. Vectors 9, 412.
Fruttero, L.L., Moyetta, N.R., Krug, M.S., Broll, V., Grahl, M.V., Real-Guerra, R., Stanisçuaski, F., Carlini, C.R., 2017. Jaburetox affects gene expression and enzyme activities in *Rhodnius prolixus*, a Chagas' disease vector. Acta Trop. 168, 54–63.
Gacko, M., Minarowska, A., Karwowska, A., Minarowski, L., 2007. Cathepsin D inhibitors. Folia Histochem. Cytobiol. 45, 291–313.
García-González, F., Gutiérrez-Benicio, G.M., Iturriaga, G., Raya-Pérez, J.C., Blanco-Labra, A., Ramírez-Pimentel, J.G., García-Gasca, T., Aguirre-Mancilla, C.L., 2017. Biocontrol of insects plague: origin of strategies and current trends. Ciencia y Tecnol. Agrop. México 5, 1–10.
Gui, Z.Z., Lee, K.S., Kim, B.Y., Choi, Y.S., Wei, Y.D., Choo, Y.M., Kang, P.D., Yoon, H.J., Kim, I., Je, Y.H., Seo, S.J., Lee, S.M., Guo, X., Sohn, H.D., Jin, B.R., 2006. Functional role of aspartic proteinase cathepsin D in insect metamorphosis. BMC Dev. Biol. 6, 49.
Guzmán-Bracho, C., 2001. Epidemiology of Chagas disease in Mexico: an update. Trends Parasitol. 17, 372–376.
Houseman, J.G., Downe, A.E.R., 1980. Endoproteinase activity in the posterior midgut of *Rhodnius prolixus* Stål (Hemiptera: Reduviidae). Insect Biochem. 10, 363–366.
Kang, T., Jin, R., Zhang, Y., Wan, H., Lee, K.S., Jin, B.R., Li, J., 2017. Functional characterization of the aspartic proteinase cathepsin D in the beet armyworm (*Spodoptera exigua*). Gene 617, 1–7.
Kappaun, K., Piovesan, A.R., Carlini, C.R., Ligabue-Braun, R., 2018. Ureases: historical aspects, catalytic, and non-catalytic properties - a review. J. Adv. Res. 13, 3–17.
Krug, M.S., 2016. A UDP-N-acetilglicosamina pirofosforilase de *Rhodnius prolixus* como possível alvo da ação do jaburetox. Universidade Federal do Rio Grande do Sul, Porto Alegre, RS, Brazil. https://lume.ufrgs.br/handle/10183/150717.
Leyria, J., Fruttero, L.L., Nazar, M., Canavoso, L.E., 2015. The rol of DmCatD, a cathepsin D-like peptidase and acid phosphatase in the process of folicular atresia in *Dipetalogaster maxima* (Hemiptera: Reduviidae), a vector of Chagas' disease. PLoS One 10, e0130144.
Leyria, J., Fruttero, L.L., Ligabue-Braun, R., Defferrari, M.S., Arrese, E.L., Soulages, J.L., Settembrini, B.P., Carlini, C.R., Canavoso, L.E., 2018. DmCatD, a cathepsin D-like peptidase of the hematophagous insect *Dipetalogaster maxima* (Hemiptera: Reduviidae): purification, bioinformatic analyses and the significance of its interaction with lipophorin in the internalization by developing oocytes. J. Insect Physiol. 105, 28–39.
Martinelli, A.H.S., Lopes, F.C., Broll, V., Defferrari, M.S., Ligabue-Braun, R., Kappaun, K., Tichota, D.M., Fruttero, L.L., Moyetta, N.R., Demartini, D.R., Postal, M., Medeiros-Silva, M., Becker-Ritt, A.B., Pasquali, G., Carlini, C.R., 2017. Soybean ubiquitous urease with purification facilitator: an addition to the moonlighting studies toolbox. Process Biochem. 53, 245–258.
Moyetta, N.R., Broll, V., Perin, A.P.A., Uberti, A.F., Coste Grahl, M.V., Staniscuaski, F., Carlini, C.R., Fruttero, L.L., 2017. Jaburetox-induced toxic effects on the hemocytes of *Rhodnius prolixus* (Hemiptera: Reduviidae). Comp. Biochem. Physiol. C Toxicol. Pharmacol. 200, 17–26.
Mulinari, F., Staniscuaski, F., Bertholdo-Vargas, L.R., Postal, M., Oliveira-Neto, O.B., Rigden, D.J., Grossi-de-Sá, M.F., Carlini, C.R., 2007. Jaburetox-2Ec: an insecticidal peptide derived from an isoform of urease from the plant *Canavalia ensiformis*. Peptides 28, 2042–2050.
Núñez, J.A., Segura, E.L., 1987. Rearing of Triatominae. In: Brenner, R.R., Stoka, A.M. (Eds.), Chagas' Disease Vectors, vol. 2. CRC Press, Florida, pp. 31–40.
Padilha, M.H.P., Pimentel, A.C., Ribeiro, A.F., Terra, W.R., 2009. Sequence and function of lysosomal and digestive cathepsin D-like proteinases of *Musca domestica* midgut. Insect Biochem. Mol. Biol. 39, 782–791.
Park, S.H., Raines, R.T., 1997. Green fluorescent protein as a signal for protein-protein interactions. Protein Sci. 6, 2344–2349.
Perin, A.P.A., 2018. Jaburetox, peptídeo derivado de ureases: efeitos sobre as vias enzimáticas da barata *Nauphoeta cinerea*. Universidade Federal do Rio Grande do Sul, Porto Alegre, RS, Brazil. https://lume.ufrgs.br/handle/10183/187227.
Pimentel, A.C., Fuzita, F.J., Palmisano, G., Ferreira, C., Terra, W.R., 2017. Role of cathepsins D in the midgut of *Dysdercus peruvianus*. Comp. Biochem. Physiol. B Biochem. Mol. Biol. 204, 45–52.
Saikhedkar, N., Summanwar, A., Joshi, R., Giri, A., 2015. Cathepsins of lepidopteran insects: aspects and prospects. Insect Biochem. Mol. Biol. 64, 51–59.
Salazar-Schettino, P.M., Rojas-Wastavino, G.E., Cabrera-Bravo, M., Bucio-Torres, M.I., Martínez-Ibarra, J.P., Monroy-Escobar, M.C., Rodas-Retana, A., Guevara-Gómez, Y., Vences-Blanco, M.O., Ruiz-Hernández, A.L., Torres-Gutiérrez, E., 2010. A revision of thirteen species of Triatominae (Hemiptera: Reduviidae) vectors of Chagas disease in Mexico. J. Selva Andina Res. Soc. 1, 57–80.
Santiago, P.B., de Araújo, C.N., Motta, F.N., Praça, Y.R., Charneau, S., Bastos, I.M., Santana, J.M., 2017. Proteases of haematophagous arthropod vectors are involved in blood-feeding, yolk formation and immunity - a review. Parasit. Vectors 10, 79.
Schaub, G.A., 2009. Interactions of Trypanosomatids and Triatomines. In: Simpson, S.J., Casas, J. (Eds.), Advances in Insect Physiology. Academic Press, London, pp. 177–242.
Staniscuaski, F., Carlini, C.R., 2012. Plant ureases and related peptides: understanding their entomotoxic properties. Toxins (Basel) 4, 55–67.
Staniscuaski, F., Te Brugge, V., Carlini, C.R., Orchard, I., 2010. Jack bean urease alters serotonin-induced effects on *Rhodnius prolixus* anterior midgut. J. Insect Physiol. 56, 1078–1086.
Stoka, V., Turk, V., Turk, B., 2016. Lysosomal cathepsins and their regulation in aging and neurodegeneration. Ageing Res. Rev. 32, 22–37.
Zhang, Z., Liu, Z., Chen, J., Yi, J., Cheng, J., Dun, W., Wei, H., 2018. Resveratrol induces autophagic apoptosis via the lysosomal cathepsin D pathway in human drug-resistant K562/ADM leukemia cells. Exp. Ther. Med. 15, 3012–3019.